AIP | Review of Scientific Instruments

Note: A 4 ns hardware photon correlator based on a general-purpose field-programmable gate array development board implemented in a compact setup for fluorescence correlation spectroscopy

Stanislav Kalinin, Ralf Kühnemuth, Hayk Vardanyan, and Claus A. M. Seidel

Citation: Rev. Sci. Instrum. **83**, 096105 (2012); doi: 10.1063/1.4753994
View online: http://dx.doi.org/10.1063/1.4753994
View Table of Contents: http://rsi.aip.org/resource/1/RSINAK/v83/i9
Published by the American Institute of Physics.

Note: A 4 ns hardware photon correlator based on a general-purpose field-programmable gate array development board implemented in a compact setup for fluorescence correlation spectroscopy

Stanislav Kalinin,[a] Ralf Kühnemuth, Hayk Vardanyan, and Claus A. M. Seidel[a]
Institut für Physikalische Chemie, Lehrstuhl für Molekulare Physikalische Chemie, Heinrich-Heine-Universität, Universitätsstraße 1, Geb. 26.32.02, 40225 Düsseldorf, Germany

(Received 2 July 2012; accepted 5 September 2012; published online 21 September 2012)

We present a fast hardware photon correlator implemented in a field-programmable gate array (FPGA) combined with a compact confocal fluorescence setup. The correlator has two independent units with a time resolution of 4 ns while utilizing less than 15% of a low-end FPGA. The device directly accepts transistor-transistor logic (TTL) signals from two photon counting detectors and calculates two auto- or cross-correlation curves in real time. Test measurements demonstrate that the performance of our correlator is comparable with the current generation of commercial devices. The sensitivity of the optical setup is identical or even superior to current commercial devices. The FPGA design and the optical setup both allow for a straightforward extension to multi-color applications. This inexpensive and compact solution with a very good performance can serve as a versatile platform for uses in education, applied sciences, and basic research. © *2012 American Institute of Physics*. [http://dx.doi.org/10.1063/1.4753994]

Fluorescence correlation spectroscopy (FCS)[1,2] is a powerful method to study diffusion and dynamics of biomolecules.[3–6] Fluctuations of the fluorescence signal $F(t)$ are characterized by auto- or cross-correlation functions $G_{ij}(t_c)$

$$G_{ij}(t_c) = \langle F_i(t + t_c)F_j(t)\rangle / (\langle F_i(t)\rangle \langle F_j(t)\rangle), \quad (1)$$

where t_c is the correlation (or lag) time, and subscripts i and j refer to distinct detection channels. For calculation of correlation functions, hardware photon correlators are often employed.[7] Nowadays, real-time software correlation is also possible,[8–11] provided that data acquisition hardware with sufficient time resolution is available. However, in any case, a dedicated data acquisition or processing board is typically required to build even a simple FCS setup.

In this work, we propose a field-programmable gate array (FPGA)-based implementation of a hardware photon correlator. Specifically, it is based on a general-purpose Xilinx SP605 evaluation board (Xilinx, USA) equipped with a value-line Spartan 6 FPGA chip (XC6SLX45T). Photon detectors can be directly connected to the SP605 board requiring no additional custom-built hardware. Test measurements of fluorescence fluctuations of Rhodamine 110 show that the time resolution of 4 ns is easily achieved in practice. In this respect, our design is comparable with "fast" versions of commercial devices, such as the ALV 6010/200. Two correlator units utilize less than 15% of the FPGA's resources, which suggests that the design should fit even into low-end FPGAs. Alternatively, more correlators can be implemented in parallel without sacrificing time resolution, which is for instance useful for FCS in combination with Förster resonance energy transfer (FRET). Additional features of our correlator include a real-time display of photon count rates, and a display of the intensity trace with millisecond time resolution. FPGA firmware and operating software are available from the authors (http://www.mpc.hhu.de/software).

While this manuscript was in preparation, Mocsár *et al.*[12] published an independent implementation of an FPGA correlator based on a National Instruments 7833R board. The design of Mocsár *et al.* is optimized for computing very large number of correlation functions; however, this feature is implemented at the cost of time resolution (100 ns for single curve, lower for multiple curves). Thus, our approach is rather complementary to that of Mocsár *et al.*'s, being optimized for time resolution, low FPGA utilization (see supplementary material, Table II),[25] and applications such as confocal detection of freely diffusing molecules.

Performance of the correlator is demonstrated using a compact home-built optical setup employing only the minimum of required optical components, ensuring maximized optical throughput and stability of alignment.

Our photon correlator has a classical multi-tau architecture, as described in detail previously[8,10,13] (see also supplementary material, Sec. 4).[25] Specifically, it has 28 internal time cascades, each consisting of 8 equally spaced time bins. The time bin width for the first two cascades is $\Delta t_c = 4$ ns, whereas it doubles for every next cascade starting from the third one. The initial part of the correlation function (~4.3 s) is thereby calculated internally using 224 time bins. Every 268 ms (synchronously with updating the last cascade), current states of all photon pair counters, total number of registered photons, and state of the last time bin are transferred to a personal computer (PC) using the provided universal serial bus (USB) (virtual serial port) interface. Higher cascades (here up to 128.8 s correlation time) are processed on the PC. These data are updated at most once per received frame, thus generating only a minimal load on the PC. To compute FCS

[a]Authors to whom correspondence should be addressed. Electronic addresses: stanislav.kalinin@uni-duesseldorf.de and cseidel@hhu.de.

curves, normalization is performed according to Eq. (2),

$$G_{ij}(t_c) = N_{pairs}(t_c)/[S_i S_j(t_{max} - t_c)\Delta t_c]. \quad (2)$$

In Eq. (2), $N_{pairs}(t_c)$ is the number of photon pairs accumulated for the time bin t_c, S_i and S_j are the average signals in channels i and j, respectively, t_{max} is the total experiment time, and Δt_c is the bin width for t_c.

The detectors must be connected to the "USER_SMA_GPIO_N" and "USER_SMA_GPIO_P" inputs of the SP605, which by design form a differential input. This can potentially result in distortion of the signal and crosstalk between the channels. We found that for 3.3 V input signals (e.g., from modern single photon avalanche photodiodes), 6 dB attenuators are sufficient to reduce crosstalk and other artifacts below detection limits (see test measurements below). For other signal levels and/or pulse shapes, optimal conditions may vary.

The inputs are sampled with an effective frequency of 500 MHz. The dead time is artificially set to 16 ns for each channel to avoid false detections due to, e.g., pulse overshoot. There is no dead time between the channels and $G(t_c = 0)$ is also calculated in the case of cross-correlation. The maximum count rate is mainly limited by the size of photon pair counters, which should not overflow more than once per transmitted frame (268 ms). We estimate that this could happen at >16 MHz per channel (average over 268 ms), which is well above optimal count rates of modern single photon detectors.

At first we correlated a pseudorandom test signal generated within the same FPGA chip using the linear feedback shift register algorithm.[14] We simulated interconversion of two states "1" and "2," for which we expect an exponential term in the correlation function. The fit of the computed correlation curve recovers expected[15] parameters with an accuracy of <0.3% (see supplementary material, Sec. 1 for details).[25]

Next, FCS measurements of Rhodamine 110 (Rh110) diffusion and photophysics were performed using a home-built confocal setup (Fig. 1). The excitation source is a tunable Ar-ion laser (35-LAP-431-220, Melles-Griot, Bensheim, Germany) set to 496 nm and coupled via single mode fiber (Schäfter & Kirchhoff, Hamburg, Germany) to a modular system consisting of galvanized aluminum cubes connected via dove-tail adapters. The main dichroic (BS 500, AHF Tübingen, Germany) is mounted on a micrometer driven rotation and tilt manipulator inside the first cube. The objective (UPlanSApo 60x/1.2w, Olympus Hamburg, Germany) is attached to a z-micrometer (SM1Z, Thorlabs Dachau, Germany) at the exit port. A tube lens (f = 160 mm achromatic lens, Linos, Göttingen, Germany) focuses the fluorescence light leaving the second exit port onto a pinhole (Plano Wetzlar, Germany), which is mounted on an 8-position wheel. Pinhole sizes can be varied between 25 μm and 5 mm (70 μm was used in the presented experiments). The spatially filtered light is then collimated by a second lens (f = 100 mm achromatic lens, Linos) before being divided by a polarizing beam splitter (TSWP 633, Linos). After passing bandpass filters (HC525/39, AHF) to remove scattered laser light and limit the detected fluorescence range, the two beams are finally focused by two plano-convex lenses (f = 10 mm, Linos) onto two single photon avalanche diodes (PD200A, MPD Bolzano, Italy or PerkinElmer SPCM AQR-14/AQRH-14). Detectors are attached via xy-micrometer manipulators. All optical components are broadband AR coated and can be exchanged quickly. The modular design allows for easy extension, i.e., to set up four, six, or eight detection channels to record multiparameter data (polarization and various spectral ranges). The sensitivity of the whole setup was found to be at least as sensitive as commercial microscopes like the Olympus IX71 equipped with equivalent detectors.

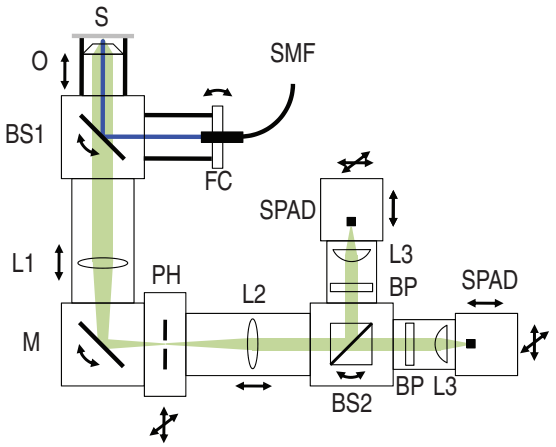

FIG. 1. Schematic drawing of the FCS setup used to perform test measurements. BS1: dichroic beamsplitter; BS2: polarizing beamsplitter; L1: tube lens f = 160 mm; L2: collimating lens f = 100 mm; L3: lens f = 10 mm; SMF: single mode fiber; FC: fiber coupler with 2-axis tilt; O: objective; S: sample plate; M: broadband mirror; PH: pinhole on 8 position wheel; BP: band pass filter; SPAD: single photon avalanche diode.

In Fig. 2, the FCS curve generated using our SP605-based design is compared with that obtained using a commercial ALV 6010/200 correlator with a specified time resolution of 5 ns. In the ~100 ns–1 s range, the curves are hardly distinguishable. At shorter correlation times the photon antibunching term[16] is slightly more pronounced in the curve computed using our correlator. We then fitted the correlation curves using Eq. (3), which accounts for translational diffusion, triplet and reaction kinetics, and photon antibunching

$$G(t_c) = 1 + \frac{1}{N}\left(\frac{1}{1 + t_c/t_d}\right)\left(\frac{1}{1 + t_c/[(z_0/\omega_0)^2 t_d]}\right)^{1/2} \times (1 - T + T\exp(-t_c/t_T)) \times (1 - K + K\exp(-t_c/t_K)) \times (1 - \exp(-t_c/t_A)). \quad (3)$$

In Eq. (3), N is an average number of bright molecules in the detection volume, t_d is the diffusion time, z_0/ω_0 is aspect ratio of the confocal volume, T is the equilibrium fraction of the triplet state, t_T is the triplet relaxation time, and t_A is the antibunching time. The second kinetic term with an amplitude K and a characteristic time t_K is caused by saturation and complex triplet and/or radical kinetics at high irradiance.[17,18] Detailed investigation of this effect and its origin is beyond the scope of this work.

The fitted parameters for the FCS curves generated using our design and the ALV 6010/200 agree typically within a few percent (see figure text for details). In particular, N and t_D show almost perfect agreement (N: 0.4%; t_D: 0.2%). The

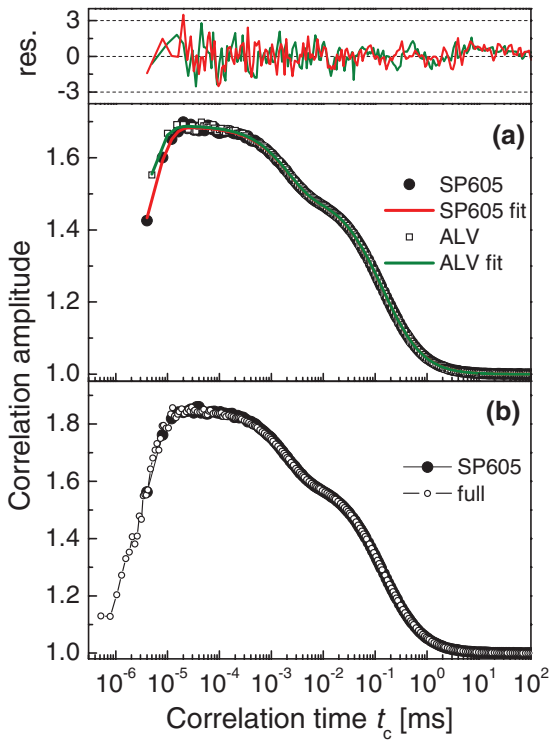

FIG. 2. (a) Comparison of the FCS curves of Rhodamine 110 generated by ALV 6010/200 (□) and the SP605-based correlator presented in this work (●). The curves are fitted by Eq. (3) with the following parameters: ALV: $N = 1.450$; $t_D = 0.144$ ms; $z_0/\omega_0 = 4.1$; $T = 0.274$; $t_T = 2.03$ μs; $K = 0.217$; $t_K = 0.591$ ms; $t_A = 3.1$ ns; SP605: $N = 1.455$; $t_D = 0.144$ ms; $z_0/\omega_0 = 4.0$; $T = 0.272$; $t_T = 2.03$ μs; $K = 0.186$; $t_K = 0.52$ ms; $t_A = 4.0$ ns. Weighted residuals are shown above. (b) Comparison with the FCS curve calculated by software correlation of photon traces recorded with TCSPC cards (○). In all cases, two cross-correlation functions (detector1→detector2 and detector2→detector1) were calculated and the average was taken. In plot (b), the curves were measured with slightly different concentrations of Rh110 and were scaled to the same amplitude. The mean irradiance was ca. 50 kW/cm^2 (450 μW at the objective).

deviations can be attributed to limited statistics of the measurements and to instability of the fit with respect to K and t_K because this process is slower than diffusion. Weighted residuals (Fig. 2(a), upper panel) show no features specific for either curve.

To ensure that the observed anticorrelation in the ns range is not due to an artifact, we recorded photon traces with picosecond time resolution using two time-correlated single-photon counting (TCSPC) cards (SPC832, Becker & Hickl, Germany) on the same experimental setup. Then we performed full software correlation of the recorded signals.[10] Figure 2(b) shows that our FCS curve agrees very well with the computed full correlation curve over the whole time range. This comparison convincingly demonstrates that the electronic time resolution of 4 ns is readily achieved in practice.

We presented a free implementation of a fast hardware correlator with features and performance similar to current commercial devices. To our knowledge, significantly better (sub-ns) time resolution can be achieved only by using high-end electronics with TCSPC capabilities (for instance, Becker & Hickl SPC series or DPC-230; PicoQuant PicoHarp or HydraHarp modules). Considering the low cost of the SP605 board and of the presented compact FCS setup, and also the fact that it can be easily extended to more than two detection channels and several parallel correlator units, our design should find more uses in research, general analytic applications, and education. An increasing number of applications of FCS has been reported for life[19–21] and material sciences.[22,23] The mobility of proteins and DNA- or RNA-fragments within the cytosol or other cell organelles belong to the most prominent measurement parameters of intracellular measurements.[24] Numerous studies are also devoted to the analysis of molecular (e.g., ligand receptor) interactions or translocation processes.[23] Therefore, flexible and low cost instrumentation[25] with high performance will facilitate the use of FCS for even more applications.

We are grateful to Dr. Suren Felekyan and to Denis Dörr for valuable discussions and help with measurements. C.S. thanks the German Science Foundation (SE 1195/13-1) and the EU (FP7-Health-2007-A-201837) for funding during this work.

[1] D. Magde, E. L. Elson, and W. W. Webb, Phys. Rev. Lett. **29**, 705 (1972).
[2] R. Rigler, Ü. Mets, J. Widengren, and P. Kask, Eur. Biophys. J. **22**, 169 (1993).
[3] P. Schwille, F. J. Meyer-Almes, and R. Rigler, Biophys. J. **72**, 1878 (1997).
[4] M. Branden, T. Sanden, P. Brzezinski, and J. Widengren, Proc. Natl. Acad. Sci. U.S.A. **103**, 19766 (2006).
[5] D. Nettels, I. V. Gopich, A. Hoffmann, and B. Schuler, Proc. Natl. Acad. Sci. U.S.A. **104**, 2655 (2007).
[6] C. Eggeling, C. Ringemann, R. Medda, G. Schwarzmann, K. Sandhoff, S. Polyakova, V. N. Belov, B. Hein, C. von Middendorff, A. Schonle, and S. W. Hell, Nature (London) **457**, 1159 (2009).
[7] K. Bacia, S. A. Kim, and P. Schwille, Nat. Methods **3**, 83 (2006).
[8] D. Magatti and F. Ferri, Rev. Sci. Instrum. **74**, 1135 (2003).
[9] M. Wahl, I. Gregor, M. Patting, and J. Enderlein, Opt. Express **11**, 3583 (2003).
[10] S. Felekyan, R. Kühnemuth, V. Kudryavtsev, C. Sandhagen, W. Becker, and C. A. M. Seidel, Rev. Sci. Instrum. **76**, 083104 (2005).
[11] T. A. Laurence, S. Fore, and T. Huser, Opt. Lett. **31**, 829 (2006).
[12] G. Mocsár, B. Kreith, J. Buchholz, J. W. Krieger, J. Langowski, and G. Vamosi, Rev. Sci. Instrum. **83**, 046101 (2012).
[13] K. Schätzel, M. Drewel, and S. Stimac, J. Mod. Opt. **35**, 711 (1988).
[14] P. Alfke, "Efficient shift registers, LFSR counters, and long pseudo-random sequence generators," Xilinx Application Note No. 052 (1996); see http://www.xilinx.com/support/documentation/application_notes/xapp052.pdf.
[15] W. Al-Soufi, B. Reija, M. Novo, S. Felekyan, R. Kühnemuth, and C. A. M. Seidel, J. Am. Chem. Soc. **127**, 8775 (2005).
[16] Ü. Mets, *Fluorescence Correlation Spectroscopy*, Springer Series in Chemical Physics Vol. 65, edited by R. Rigler and E. L. Elson (Springer-Verlag, 2001),Chap. 16, p. 346.
[17] J. Widengren, Ü. Mets, and R. Rigler, J. Phys. Chem. **99**, 13368 (1995).
[18] J. Widengren, A. Chmyrov, C. Eggeling, P. A. Lofdahl, and C. A. M. Seidel, J. Phys. Chem. A **111**, 429 (2007).
[19] E. Haustein and P. Schwille, Annu. Rev. Biophys. Biomol. Struct. **36**, 151 (2007).
[20] Z. Petrasek and P. Schwille, J. R. Soc., Interface **6**, S15 (2009).
[21] A. Shahzad and G. Kohler, Appl. Spectrosc. Rev. **46**, 166 (2011).
[22] S. Salzinger, S. Huber, S. Jaksch, P. Busch, R. Jordan, and C. M. Papadakis, Colloid Polym. Sci. **290**, 385 (2012).
[23] W. Al-Soufi, B. Reija, S. Felekyan, C. A. M. Seidel, and M. Novo, Chem. Phys. Chem. **9**, 1819 (2008).
[24] S. R. Yu, M. Burkhardt, M. Nowak, J. Ries, Z. Petrasek, S. Scholpp, P. Schwille, and M. Brand, Nature (London) **461**, 533 (2009).
[25] See supplementary material at http://dx.doi.org/10.1063/1.4753994 for further implementation details and test measurements.